Chinese Chemical Letters 30 (2019) 1013–1016

Contents lists available at ScienceDirect

Chinese Chemical Letters

journal homepage: www.elsevier.com/locate/cclet

Communication

Direct and single-step sensing of primary ovarian cancers related glycosidases

Dan Li[1], Ling Liang[1], Yawei Tang, Linna Fu, Shehua Xiao, Quan Yuan*

Molecular Science and Biomedicine Laboratory, Institute of Chemical Biology and Nanomedicine, State Key Laboratory of Chemo/Biosensing and Chemometrics, College of Chemistry and Chemical Engineering, Hunan University, Changsha 410082, China

ARTICLE INFO

Article history:
Received 16 October 2018
Received in revised form 17 December 2018
Accepted 18 December 2018
Available online 19 December 2018

Keywords:
Black phosphorus quantum dots
Fluorescence
Sensing
β-Galactosidase
Inner filter effect

ABSTRACT

High sensitive, accurate detection for tumor-associated overexpressed enzyme activity is highly significant for further understanding enzyme function, discovering potential drugs, and early diagnosis and prevention of diseases. In this work, we developed a facile, direct and single-step detection platform for primary ovarian cancers related glycosidase activity based on the inner filter effect (IFE) between glycosidase catalytic product and black phosphorus quantum dots (BPQDs). Highly fluorescent BPQDs were successfully synthesized from bulk black phosphorus by a simple liquid exfoliation method. Under the catalysis of β-galactosidase, *p*-nitrophenyl-β-D-galactopyranoside (PNPG) was transformed into *p*-nitrophenol (PNP) and β-D-galactopyranoside. Meanwhile, the absorption of catalytic product PNP greatly overlapped with the excitation and emission spectra of fluorescent BPQDs, leading to the fluorescence quenching of BPQDs with a high quenching efficiency. The proposed sensing strategy provided a low detection limit of 0.76 U/L, which was 1 – 2 orders of magnitude lower than most unmodified sensing platforms. D-Galactal was selected as the inhibitor for β-galactosidase to further assess the feasibility of screening potential inhibitors. The fluorescence recovery of BPQDs suggests that the unmodified sensing platform is feasible to discover potential drugs of β-galactosidase. Our work paves a general way in the detection of glycosidase activity with fluorescent BPQDs, which can be promising for glycosidase-related disease diagnosis and pathophysiology elucidation.

Glycosidases are enzyme that closely related to various important biological processes due to their effective and complicated catalytic hydrolysis of glycosidic linkages [1]. More importantly, it was discovered that glycosidase acted a pivotal part in the pathology of several disease states including Gaucher and Parkinson's diseases [2]. Among these known glycosidases, β-galactosidase (β-Gal) has been demonstrated as a lysosomal exoglycosidase for the removal of galactose residues from various substrates, such as gangliosides, glycoproteins, sphingolipids, and keratin sulfate [3]. In addition, the high expression of β-Gal has been associated with progression of various cancers [4], in particularly with that of ovarian and colorectal cancer [5–8]. Meanwhile, it is also a molecular target for visualizing peritoneal metastasis from ovarian cancer [9]. Although various fluorometric assays have been developed for β-Gal activity [10–16], these approaches usually suffer from some drawbacks including high absorption of biomolecules, complicated synthesis process or surface modification, and substantially hinder their practical application in clinical test and biological research. Therefore, the development of facile, direct and single-step β-Gal detection could be beneficial for better understand glycosidases function and screen potential inhibitors.

Black phosphorus, a metal-free 2D layered semiconductor, exhibits a thickness-dependent tunable band gap ranging from about 0.3 eV (bulk) to 2.0 eV (monolayer) [17–19]. Few-layer black phosphorus demonstrate highly layer-dependent photoluminescence from mid-infrared to near-infrared wavelengths through tunable band gaps, making black phosphorus a promising novel nanomaterial for the development of optoelectronic devices [20–22], nanoelectronic devices [23–26] and gas sensors [25,27,28]. Recently, Sang *et al.* reported that a stable blue emitting black phosphorus quantum dots (BPQDs) could be prepared in chloroform by a simple sonication-assisted liquid-phase exfoliation of black phosphorus flakes in the ambient atmosphere [29]. Besides, Xian *et al.* reported that BPQDs with significant green fluorescence were successfully synthesized from bulk black phosphorus by sonication-assisted solvothermal method [30]. However, exploration of the potential biosensing

* Corresponding author.
E-mail address: yuanquan@whu.edu.cn (Q. Yuan).
[1] These authors contributed equally to this work.

https://doi.org/10.1016/j.cclet.2018.12.022

applications of black phosphorus remains limited, especially in the field of cancers related glycosidases. The development of a novel biosensor platform based on the superior optical properties of BPQDs is especially important and highly anticipated for glycosidase activity detection, discovering potential new drugs, cancer diagnosis and therapy.

In our work, a convenient, direct and single-step detection platform was firstly designed for glycosidase activity detection. The designed sensing mechanism of this strategy through the inner filter effect (IFE) of *p*-nitrophenol (PNP) on the fluorescence of BPQDs was illustrated in Scheme 1. The BPQDs with strong blue fluorescence were obtained by environmentally friendly liquid-exfoliation method [31–33]. The maximum excitation and emission wavelengths of the BPQDs were at 370 and 447 nm, respectively. In the presence of specific glycosidase, the glycoconjugate of PNP can be rapidly hydrolyzed to the corresponding glucose and PNP. UV–vis absorption spectrum of PNP has a good overlap with the excitation and emission spectra of the exfoliated BPQDs, leading to efficient fluorescence quenching of BPQDs. As an important indicator in progression of various cancers, the investigation of β-Gal inhibitor is of great significance [34]. Therefore, the proposed sensing platform was also applied to investigate β-Gal inhibitors to drug discovery. The fluorescence recovery of BPQDs suggests that the unmodified sensing platform is feasible to discover potential drugs of β-galactosidase. Thus, the proposed sensing method was proven to enjoy the merits of superior sensitivity, direct and single-step, showing a great promising in clinic diagnostic and drug screening.

BPQDs were synthesized in *N*-methyl-2-pyrrolidone by a liquid ultrasonication exfoliation method [31]. The as-obtained BPQDs were thoroughly characterized by transmission electron microscopy (TEM) and atomic force microscopy (AFM). Figs. 1A and B revealed the uniform morphology of the BPQDs, and the high-resolution TEM (HRTEM) image (Fig. 1C) shows lattice fringes of 0.21 nm, which was ascribed to the (014) plane of the black phosphorus crystal [35,36]. Statistical analysis on TEM images demonstrated that the average lateral size was 2.9 ± 0.4 nm (Fig. 1D). AFM image indicated that BPQDs possessed a thickness ranging from ~1.0 to 1.5 nm, corresponding to $1-2$ layers. The above results clearly suggest that ultrasmall BPQDs successfully prepared by the liquid exfoliation method.

UV-vis absorption and fluorescence emission spectrum were carried out to investigate the optical properties of BPQDs. The as-prepared BPQDs displayed a maximum absorption at around 230 nm (Fig. S1 in Supporting information). As shown in Fig. 2A, the emission peak was red shifted from 400 nm to 502 nm with the excitation wavelength varying from 300 nm to 420 nm, which revealed the excitation-dependent fluorescence emission of BPQDs. The maximum emission was located at 447 nm with excitation of 370 nm. The above tuneable emission suggested that

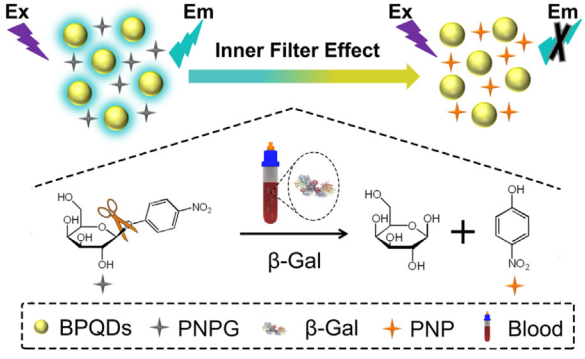

Scheme 1. Schematic illustration of IFE-based BPQDs sensor for detection of β-Gal.

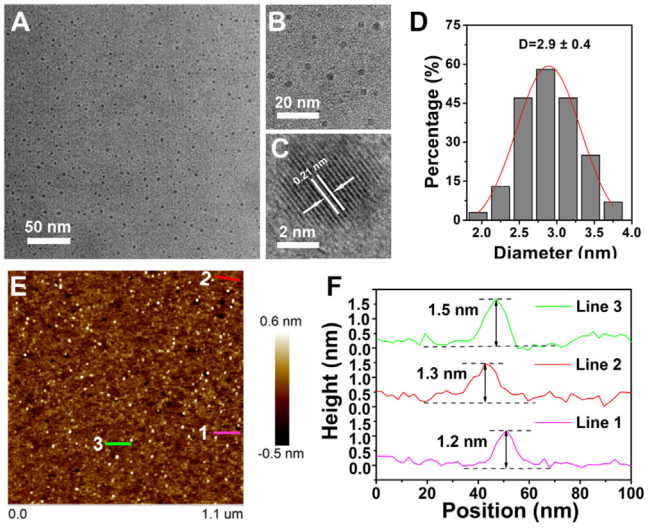

Fig. 1. TEM image (A), magnified TEM image (B) and HRTEM image (C) of BPQDs. (D) Statistical analysis of the size of BPQDs measured from TEM images. (E) AFM image and (F) corresponding height analysis of BPQDs.

BPQDs with different sizes have varied fluorescence characteristics or exist different emissive sites on the surfaces of the material [30,37,38]. The BPQDs fluorescent probe used in practical sensing applications must be of sufficient stability toward ambient environments, therefore, the influences of fluorescence intensity of BPQDs in different buffer and pH was firstly investigated. As shown in Fig. 2B, no change of the fluorescence intensity was observed when the fluorescent probe was dissolved in different buffer (PBS, HEPES, Tris-HCl and H_2O). The fluorescence intensity of the as-prepared BPQDs was relatively stable over pH values ranging from 2 to 11 (Fig. 2C), indicating the stability of the BPQDs fluorescent probe. To further assess the photostability, the fluorescence intensity of BPQDs upon radiation with a UV light (370 nm) was monitored. Fig. 2D shows the fluorescence intensity remained almost constant under UV light for 1 h. These results thus suggest that BPQDs have good stability in different conditions, implying that BPQDs are particularly valuable for real applications in biosensing.

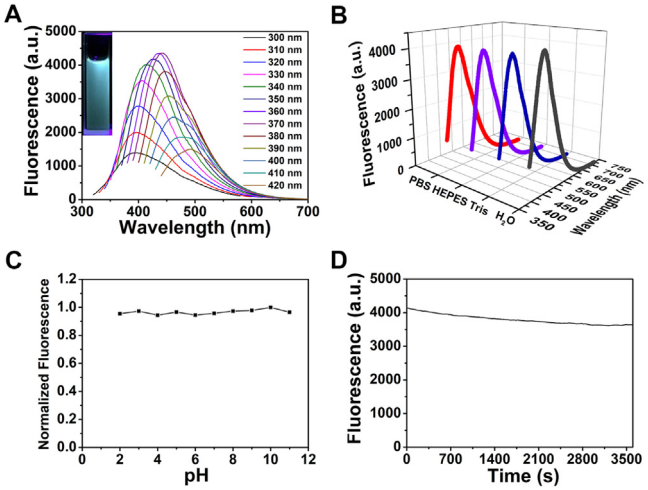

Fig. 2. (A) Photoluminescence (PL)/Fluorescence spectra of BPQDs at different excitation wavelengths within the 300–450 nm range. (B) Fluorescence intensity of BPQDs at different buffer. (C) Fluorescence intensity of BPQDs at different pH values. (D) Fluorescence intensity variation of BPQDs as a function of time under 370 nm light illumination.

We fabricated a fluorescence sensing platform based on IFE for direct and single-step detection of β-Gal. In this reaction system, BPQDs and PNP were selected as fluorescence measure indicators and fluorescence quenchers, respectively. The absorption peak of hydrolysate PNP has a strong absorption (405 nm) in the range of 370–450 nm (Fig. 3A), which was greatly overlapped with the excitation and emission spectra of BPQDs. Obviously, since PNP could shield both the excitation light and emission light from BPQDs, the fluorescence intensity of BPQDs could be effectively quenched, suggesting the IFE between BPQDs and PNP. The UV–vis absorption of the reaction solution with various β-Gal levels was also measured based on the above IFE mechanism. The absorptions at 310 and 405 nm were gradually decreased and increased, respectively (Fig. 3B). Meanwhile, the colours of reaction solution obviously changed from colourless to yellow (Fig. 3C). Therefore, BPQDs-based fluorescence method was able to successfully use for the detection of β-Gal. The fluorescence quenching mechanism was further explored by time-resolved florescence spectrometry. As shown in Fig. 3D, the fluorescence lifetime of BPQDs has no obvious change in the absence and presence of PNP. In addition, the IFE was considered to have no effect on the lifetime of the fluorophore [39]. The results indicated that the fluorescence quenching of BPQDs ascribed to IFE.

To improve the sensitivity of BPQDs detection, reaction temperature, reaction time and the concentration of PNP were systematically optimized, respectively. As observed from Figs. S2–S4 (Supporting information), 37 °C, 40 min and concentration of PNP (150 μmol/L) were selected as the optimal conditions. Under the optimum conditions, the fluorescence spectra were recorded after adding various concentrations of β-Gal. The fluorescence intensity of BPQDs decreased gradually with the increasing β-Gal concentrations (Fig. 4A). A good linear relationship between the relative fluorescence intensity and the concentration of β-Gal was obtained in the range of 5–30 U/L (Fig. 4B). The quantities' results show that the detection limit of β-Gal was as low as 0.76 U/L (S/N = 3). Furthermore, two additional concentrations of PNPG were used to investigate the effect of the concentration of PNPG on the analytical performance of the β-Gal assay. As shown in Figs. S5 and S6 (Supporting information), PNPG substrate with 100 μmol/L and 200 μmol/L also indicated good performance in assessing the detection of β-Gal level. Their limits of detection were calculated to

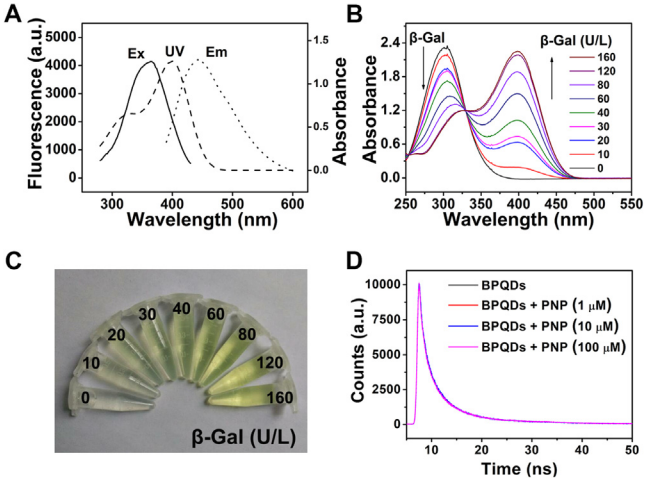

Fig. 3. (A) UV–vis spectra of PNP (dash), excitation (solid) and emission spectra (dot) of BPQDs. (B) UV–vis absorption spectrum of BPQDs + PNPG in the presence of β-Gal with various concentrations (from top to bottom 0, 10, 20, 30, 40, 60, 80, 120, and 160 U/L). (C) The photograph of BPQDs + PNPG in the presence of β-Gal with various concentrations. (D) Fluorescence lifetime of BPQDs in the presence of different concentration of PNP (1, 10, 100 μmol/L).

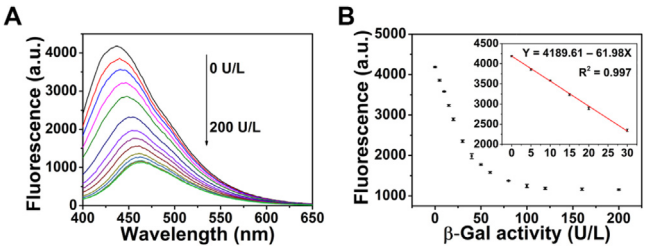

Fig. 4. (A) The fluorescence spectra of BPQDs + PNPG with different levels of β-Gal (from top to bottom 0, 5, 10, 15, 20, 30, 40, 50, 60, 80, 100, 120, 160, and 200 U/L). (B) The dependence of fluorescence intensity on the concentration of β-Gal. Inset of B is the linear plot of fluorescence intensity *versus* concentration of β-Gal over the range of 5–30 U/L.

be 0.6 and 0.7 U/L for β-Gal, respectively, demonstrating that the amount of PNPG used in the assays substantially exerts no impact on the good reproducibility and stability. Compared to previously reported results with β-Gal fluorescence measurements, our proposed IFE-based detection method that using BPQDs as fluorescent probe provided a lower detection limit (Table S1 in Supporting information) [8,10], which was 1 – 2 orders of magnitude lower than most unmodified sensing platforms. As a result, the developed method is a convenient, high sensitive and accurate detection platform for glycosidase activity detection.

To evaluate the specificity of BPQDs for detection of β-Gal, we investigated the fluorescence response of the sensing system to various interfering agents (Cu^{2+}, Fe^{2+}, K^{+}, Mg^{2+}, Na^{+}, Zn^{2+}, DL-α-amino acid, L-cystine, phenylalanine, L-tyrosine, L-valine, L-isoleucine, L-glutamic acid, glycine, ALP, BSA, GSH, and GOX). The fluorescence of BPQDs was almost unchanged after adding the interfering agents. In contrast, the fluorescence of BPQDs exhibited significant decrease (Fig. 5) in the presence of β-Gal (200 U/L). Notably, the fluorescent probe is highly selective toward β-Gal compared with other interfering agents. The above results indicate that the proposed method has a high selectivity toward β-Gal and potential application for monitoring β-Gal in real samples.

The developed fluorescence sensing platform was applied to evaluate the efficiency of enzyme inhibitors. D-Galactal as a common inhibitor of β-Gal was employed for inhibiting assays. The hydrolysis of PNPG is restricted with the addition of D-galactal, which leads to the fluorescent recovery of BPQDs. Fig. 6 shows that the fluorescence recovery with the addition of increasing concentrations of the inhibitor. The equation is as follows:

$$I(\%) = \frac{F_1 - F_0}{F_B - F_0} \times 100\% \quad (1)$$

where F_B stands for the initial fluorescence intensity in absence of β-Gal, F_0 represent the fluorescence intensity in presence of β-Gal without D-galactal, and F_1 is the fluorescence intensity in the

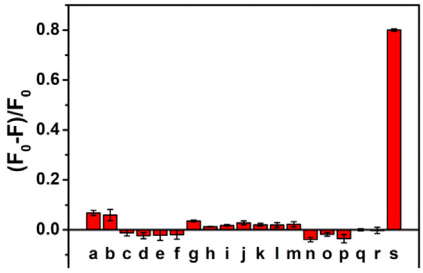

Fig. 5. Selectivity of the BPQDs fluorescent probe for β-Gal. F_0 and F represent the fluorescence intensity of the sensing system without and with β-Gal, respectively. (a) $CuCl_2$, (b) $FeSO_4$, (c) KCl, (d) $MgCl_2$, (e) NaCl, (f) $ZnCl_2$, (g) D-α-amino acid, (h) L-cystine, (i) L-phenylalanine, (j) L-tyrosine, (k) L-valine, (l) L-isoleucine, (m) L-glutamic acid, (n) glycine, (o) ALP, (p) BSA, (q) GSH, (r) GOX, and (s) β-Gal.

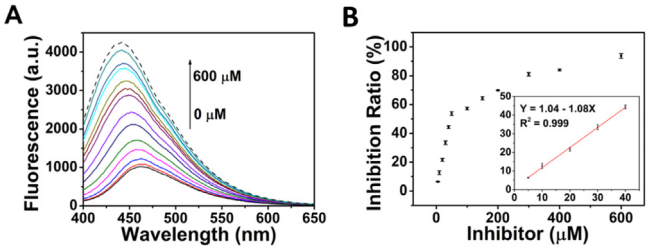

Fig. 6. (A) The fluorescence intensity of BPQDs + PNPG + β-Gal with different levels of D-galactal (0, 5, 10, 20, 30, 40, 50, 100, 150, 200, 300, 400, and 600 μmol/L). (B) The dependence of fluorescence intensity on the concentration of PNPG. Inset is the linear plot of fluorescence intensity *versus* concentration of PNPG over the range of 5–40 μmol/L.

Table 1
Measurements of β-Gal in real human serum samples.

Samples	Added β-Gal (U/L)	Found β-Gal (U/L)	Recovery (%)
1	10	9.90 ± 0.36	99
2	15	15.15 ± 0.18	101
3	20	20.61 ± 0.14	103
4	30	29.59 ± 0.34	99

presence of β-Gal with the D-galactal. The limit of detection was calculated to be 2.8 μmol/L (S/N = 3). These results indicate that our proposed method could be used to screen potential inhibitors of β-Gal.

To evaluate the feasibility of the proposed fluorescent method in real samples, we used the fluorescence sensor platform to detect β-Gal of human serum samples. The results obtained by the standard addition method were shown in Table 1. And the accuracy of the proposed approach was evaluated by determining the average recoveries of β-Gal in these serum samples. It was found that the recovery of β-Gal is in the range of 99%–103%. The relative standard deviation (RSD) was no more than 3.6%. These results indicate that the proposed fluorescent method has potential application for β-Gal detection in practical samples.

β-Galactosidase with a low detection limit of 0.76 U/L was achieved, which was 1 – 2 orders of magnitude lower than most unmodified sensing platforms. The positive results for inhibitor screening show that D-galactal could be as a reliable inhibitor for β-galactosidase, indicating the feasibility of the detection platform to screen potential inhibitors. Moreover, the proposed fluorescent method has potential application for β-Gal detection in practical samples. To conclude, our presented IFE-based method not only provides a potential platform for β-Gal sensing in clinical diagnosis and β-Gal inhibitor screening in drug discovery, but also will open a new avenue for the facile, direct and single-step β-Gal detection.

Acknowledgments

This work was supported by the National Key R&D Program of China (No. 2017YFA0208000), the National Natural Science Foundation of China (No. 21675120), Ten Thousand Talents Program for Young Talents, the Foundation for Innovative Research Groups of the National Nature Science Foundation of China (No. 21521063), and the Start-up Research Fund for Prof. Q. Yuan (Nos. 531107050973, 531109010053).

Appendix A. Supplementary data

Supplementary material related to this article can be found, in the online version, at doi:https://doi.org/10.1016/j.cclet.2018.12.022.

References

[1] D.H. Juers, B.W. Matthews, R.E. Huber, Protein Sci. 21 (2012) 1792–1807.
[2] T.D. Butters, R.A. Dwek, F.M. Platt, Chem. Rev. 100 (2000) 4683–4696.
[3] F. Vella, Biochem. Educ. 24 (1996) 65–65.
[4] D.L. Meany, D.W. Chan, Clin. Proteom. 8 (2011) 1–14.
[5] D. Asanuma, M. Sakabe, M. Kamiya, et al., Nat. Commun. 6 (2015) 6463.
[6] K. Gu, Y. Xu, H. Li, et al., J. Am. Chem. Soc. 138 (2016) 5334–5340.
[7] J. Huang, N. Li, Q. Wang, Y. Gu, P. Wang, Sensor. Actuat. B-Chem. 246 (2017) 833–839.
[8] W. Wang, K. Vellaisamy, G. Li, et al., Anal. Chem. 89 (2017) 11679–11684.
[9] S.K. Chatterjee, M. Bhattacharya, J.J. Barlow, Cancer Res. 39 (1979) 1943–1951.
[10] L. Peng, M. Gao, X. Cai, et al., J. Mater. Chem. B 3 (2015) 9168–9172.
[11] S. Trifonov, Y. Yamashita, M. Kase, M. Maruyama, T. Sugimoto, Anat. Sci. Int. 91 (2016) 56–67.
[12] R.K. Gary, S.M. Kindell, Anal. Biochem. 343 (2005) 329–334.
[13] D. Maruhn, Clin. Chim. Acta 73 (1976) 453–461.
[14] H.W. Lee, C.H. Heo, D. Sen, et al., Anal. Chem. 86 (2014) 10001–10005.
[15] C. Tang, J. Zhou, Z. Qian, et al., J. Mater. Chem. B 5 (2017) 1971–1979.
[16] M. Kamiya, D. Asanuma, E. Kuranaga, et al., J. Am. Chem. Soc. 133 (2011) 12960–12963.
[17] Z. Guo, H. Zhang, S. Lu, et al., Adv. Funct. Mater. 25 (2015) 6996–7002.
[18] H. Liu, Y. Du, Y. Deng, P.D. Ye, Chem. Soc. Rev. 44 (2015) 2732–2743.
[19] H. Liu, A.T. Neal, Z. Zhu, et al., ACS Nano 8 (2014) 4033–4041.
[20] Z. Shen, S. Sun, W. Wang, et al., J. Mater. Chem. A 3 (2015) 3285–3288.
[21] N. Youngblood, C. Chen, S.J. Koester, M. Li, Nat. Photonics 9 (2015) 247.
[22] S. Liu, S. Lin, P. You, et al., Angew. Chem. Int. Ed. 56 (2017) 13717–13721.
[23] W. Zhao, Z. Xue, J. Wang, et al., ACS Appl. Mater. Interfaces 7 (2015) 27608–27612.
[24] X. Zhang, H. Xie, Z. Liu, et al., Angew. Chem. Int. Ed. 54 (2015) 3653–3657.
[25] C. Zhu, F. Xu, L. Zhang, et al., Chem.-Eur. J. 22 (2016) 7357–7362.
[26] L. Li, Y. Yu, G.J. Ye, et al., Nat. Nanotechnol. 9 (2014) 372–377.
[27] L. Kou, T. Frauenheim, C. Chen, J. Phys. Chem. Lett. 5 (2014) 2675–2681.
[28] Z. Sofer, D. Bousa, J. Luxa, V. Mazanek, M. Pumera, Chem. Commun. 52 (2016) 1563–1566.
[29] M. Lee, Y.H. Park, E.B. Kang, et al., ACS Omega 2 (2017) 7096–7105.
[30] W. Gu, X. Pei, Y. Cheng, et al., ACS Sens. 2 (2017) 576–582.
[31] Z. Sun, H. Xie, S. Tang, et al., Angew. Chem. 127 (2015) 11688–11692.
[32] A.H. Woomer, T.W. Farnsworth, J. Hu, et al., ACS Nano 9 (2015) 8869–8884.
[33] P. Yasaei, B. Kumar, T. Foroozan, et al., Adv. Mater. 27 (2015) 1887–1892.
[34] Y.C. Lee, Biochem. Biophys. Res. Commun. 35 (1969) 161–167.
[35] R. Hultgren, N.S. Gingrich, B.E. Warren, J. Chem. Phys. 3 (1935) 351–355.
[36] Y. Zhao, H. Wang, H. Huang, et al., Angew. Chem. Int. Ed. 55 (2016) 5003–5007.
[37] H.U. Lee, S.Y. Park, S.C. Lee, et al., Small 12 (2015) 214–219.
[38] W. Gu, Y. Yan, X. Pei, et al., Sensor. Actuat. B-Chem. 250 (2017) 601–607.
[39] M. Zhang, X. Cao, H. Li, et al., Food Chem. 135 (2012) 1894–1900.